Excursion to the World of Heptacyclic Compounds Made of Azulenes and Acetylenedicarboxylates

Chen, Yi ; Lehto, Erja ; Uebelhart, Peter ; Linden, Anthony ; Hansen, Hans-Jürgen

Abstract: Azulenes and acetylenedicarboxylates react under acid catalysis (Brønsted or Lewis) and form (2aRS,8aSR)-2a,8a-dihydrocyclopenta[cd]azulene-1,2-dicarboxylates as intermediate products, which then dimerize by central bond-formation between C(2a1) and C(2'a1) and various peripheral C,C'-atoms of the dihydroazulene fragments, depending on the substituents present. The reactions are often accompanied by the formation of side-products, such as 2-(azulen-1-yl)fumarates and -maleates and others caused by H-shifts of the primary intermediates. H-Shifts between the two tetrahydrocyclopenta[cd]azulene parts of the heptacyclic structures were also found.

DOI: https://doi.org/10.1002/hlca.201500082

H15082. Excursion in the World of Heptacyclic Compounds Made of Azulenes and Acetylenedicarboxylates

by Yi Chen, Erja Lehto, Peter Uebelhart, Anthony Linden, and Hans-Jürgen Hansen

Institut für Chemie der Universität Zürich, Winterthurerstrasse 190, CH 8057 Zürich

H.-J. Hansen deceased on April 28th, 2015; correspondence should be addressed to Prof. Dr. H. Heimgartner (e-mail: heinz.heimgartner@chem.uzh.ch).

Dedicated to Klaus Hafner on the occasion of his 88th birthday

Azulenes and acetylenedicarboxylates react under acid catalysis (*Brønsted* or *Lewis*) and form as intermediate products (2a*RS*,8a*SR*)-2a,8a-dihydrocyclopenta[*cd*]azulene-1,2-dicarboxylates, which then dimerize by central bond formation between C(2a^1) and C(2'a^1) and various peripheral C,C'-atoms of the dihydroazulene fragments, depending on the substituents present. The reactions are often accompanied by the formation of side-product such as 2-(azulen-1-yl)fumarates and -maleates and others caused by H-shifts of the primary intermediates. H-shifts between the two tetrahydrocyclopenta[*cd*]-azulene parts of the heptacyclic structures were also found.

1. Introduction. – After the establishment of the structure of azulene as the non-alternating π-isomer of naphthalene by *Pfau* and *Plattner* in 1936 [1], research on azulenes became a center of interest for chemists in view of syntheses, electrophilic substitution reactions, and physiochemical as well as pharmacological behavior (*cf.* [2] and lit. cited there). A further milestone in azulene chemistry arose 40 years later when *Klaus Hafner et al.* found that heating of azulene in tetralin in the presence of dimethyl acetylenedicarboxylate (ADM) leads to the formal insertion of ADM in the C(1)–C(8a) bond of azulene, thus resulting in the formation of dimethyl heptalene-4,5-dicarboxylate [3a], the structure of which was fully established by its X-ray crystal-structure analysis [3b] (see also [4]).

Years later, we performed a detailed mechanistic analysis of the thermal transformation of azulenes with ADM into heptalene-4,5-dicarboxylates, the results of which are summarized in *Scheme 1*. There are indeed two thermal pathways for the reaction between azulenes and ADM leading to the primary intermediates of type **A** and **B** [5]. In the presence of an excess of ADM both intermediates can be trapped by a *Diels-Alder* reaction of their conjugated diene system with ADM, thus resulting in stable tetracyclic tetracarboxylates (see, *e.g.*, [6]). Moreover, the type **B** intermediates undergo a reversible thermal sigmatropic [1,5]-C shift to form **B'** structures [7][8]. Most interesting are the type **A** intermediates, the occurrence of which is based on their stable ADM cycloadducts. However, when azulenes are exposed to ADM at 30° and at pressures of 7 kbar, the primary adducts of type **A** can be isolated and characterized [9][10]. The solvent dependence of their transformation into heptalene-4,5-dicarboxylates indicates that the C(3)–C(3a) bond is cleaved heterolytically, followed by formation of 2a*H*-cyclobuta-[*c*]azulene-1,2-dicarboxylates, which then ring-opens to the observed heptalene-4,5-dicarboxylates of type **D** [10][11].

Scheme 1

Altogether, the above gives a closed mechanistic picture of the thermal reaction of azulenes with ADM under neutral conditions. Under acidic conditions, however, a new path is opened, which ends *inter alia* in the

formation of a third cycloadduct of type **C** (*Scheme 1*), which, in the most simple manner, can tautomerize to yield anellated azulene-1,2-dicarboxylates of type **E**. The following parts of this work present detailed analyses of the chemical fate of intermediates of type **C** in the presence of acids.

2. Reaction of Azulenes with Acetylenedicarboxylates under Acid Catalysis. – We published already some years ago the results of keeping a 0.39M solution of azulene (**1a**) itself in tetralin over 14 d at ambient temperature in the presence of 1.5 mol-equiv. ADM and a catalytic amount of trifluoroacetic acid (TFA; *ca.* 5 mol-% with respect to applied ADM) [12]. The most important products, which we found beside recovered **1a** (75%) by chromatographic workup, are displayed in *Scheme 2*.

Scheme 2

Fumarate (*E*)-**2a** and maleate (*Z*)-**2a** are the normally expected products of the reaction of azulenes with ADM in acidic milieu. Compound **3a** corresponds to **E**, and (*Z*)-**4a** represents the result of a concerted ene reaction of the primary intermediate **C** with ADM (*Scheme 1*). The two leading structures, heptacycles **5a** and **6a**, can be understood as dimers of **C** formed by bond formation between the central C-atoms C(2a[1]) and C(2'a[1]), as well as between C(8),C(6') in the case of **5a** or C(3),C(8') in the case of **6a**[1]).

With the focus on the formation of dimers of type **5** and **6**, we searched for more efficient acid catalysts and found in diethylaluminum chloride (Et_2AlCl; 1.4 M solution in hexane) the ideal *Lewis* acid catalyst, when applied at 0° in toluene to azulenes and ADM or other acetylenedicarboxylates (ADR; R = I = ^{i}Pr; R = B = ^{t}Bu) over 15 min or more. The results with **1a** and ADM are shown in *Scheme 3*. Beside (*E*)/(*Z*)-**2a**, dimers **5a** and **6a** are now the main products, accompanied by a third dimer **7a**, which possesses C_2 symmetry and could be distinguished therefore easily from **6a** by NMR spectroscopy in mixtures of **6a**

[1]) In the following, we will denote dimers of type **7a**, **5a** and **6a** without further ado as C(8),C(8')-, C(8),C(6')- and C(3),C(8')-dimers, respectively, since the central bond ((C(2a[1])–C(2'a[1])) is in all cases the same.

and **7a**. The structures of all three dimers followed from their ^{1}H-NMR spectra and a detailed analysis of the observed chemical shifts and ^{1}H,^{1}H coupling parameters (Table 1). Moreover, crystals of **5a** were suitable for an X-ray crystal structure analysis, which fully confirmed the structure of **5a** (Fig. 1).

Scheme 3

Table 1

Fig. 1

Most interesting are the C–C bond lengths between the two tetrahydro-cyclopenta[*cd*]azulene parts of **5a**, which are 159.0(3) (C(2a^1)–C(2'a^1)) and 160.5(3) pm (C(8)–C(6')). Both are distinctly longer than normal σ-C,C bonds, and it is also of interest to note that the central C–C bond is slightly shorter than the peripheral one (see later).

We wanted to learn more about the criteria for the formation of dimers of types **5** – **7** and investigated therefore a number of azulenes with alkyl substituents in "remote" positions, *i.e.*, in positions where no steric influence should be exerted on the formation of the primary intermediates of type **C** nor on the following bond formation between C(2a^1) and C(2'a^1) of a second molecule **C**' under acid catalysis. However, the further step, *i.e.*, the peripheral bond formation, may well be influenced by the presence of azulene substituents. The results with Me or ^{t}Bu at C(6) of the starting azulene (**1b** and **1c**, respectively) are displayed in *Scheme 4*.

Scheme 4

Indeed, all three types of dimers, which we had observed with azulene itself (*Scheme 3*), were also present in the reaction mixture of **1b** with ADM or ADI. Moreover, we found a further dimer (**8b** and **8'b**, respectively) with a single σ-bond between C(2a^1) and C(2'a^1), but a higher degree of hydrogenation, respectively, dehydrogenation of their cyclopenta[*cd*]azulene parts. We suppose that these dimers are formed in the original reaction mixture by H^+-catalyzed disproportionation of the dimers **5b** and **5'b**, respectively, initiated by cleavage of their peripheral C(8)–C(6') bond after protonation. This view is

supported by the fact that storage of **5b** in a solution of aged $CHCl_3$ overnight at room temperature led to the formation of **8b**[2]).

The structures of **6b** and **8b** were secured by X-ray diffraction analyses of suitable crystals. In another context, we already published the results of the crystal-structure determination of **6b** [13][3]). Again, one observes for **6b** a quite long central σ-bond C(2a^1)–C(2'a^1) (156.1(2) pm) and a still longer peripheral σ-bond C(3)–C(8') (161.2(3) pm). The internal H^+-catalyzed disproportionation of **5b** is of interest since it creates in **8b** on one side a 2a,4a,8a-trihydrocyclopenta[*cd*]azulen-2a^1-yl fragment and, on the side, a 8'a-hydrocyclopenta[*cd*]azulen-2'a^1-yl unit. The latter belongs to the class of 10π-homoaromatic systems, called by *L. Paquette et al*. "elassovalenes" [14] (see also lit. cited in [12]). The X-ray crystal structure of dimer **8b** revealed the presence of two independent molecules in the asymmetric unit, which differed only slightly in the relative spatial orientation of the ester groups at C(1)=C(2) and C(1')=C(2'). The stereoprojection of molecule A is displayed in *Figure 2*. It shows that all four H-atoms at the ternary C-atoms point inward in the molecule, *i.e.*, alongside the central C(2a^1)–C(2'a^1) bond, which has a length of 156.7(2) pm (A) and 157.2(2) pm (B), respectively. The torsion angle Θ(C(2a^1)–C(2'a^1)–C(8'a)–H in molecules A and B is 0.6 and 1.7°, respectively. Moreover, H–C(8'a) points in A and B towards the π-bonds of the opposite seven-membered ring.[4])

Figure 2

---

[2]) Indeed, traces of **8b** were also found in the ^{1}H-NMR spectra of pure **5b** in normally stored $CDCl_3$ (see also later).

[3]) For a stereoprojection of the structure, see *Fig. 2* displayed in [13].

[4]) AM1 calculations of the analog of **8b**, released from the four ester groups to restrict the conformational freedom of the molecule to that of the central σ-bond C(2a^1)–C(2'a^1), gave, as expected, three minima with $\Delta H_f°$ = 174.12, 176.18, and 176.90 Kcal·mol^{-1}. The conformation with the lowest value corresponds to that found for A and B in the crystal structure of **8b** and discussed above. The other two conformations show H–C(8'a) pointing towards the π-system of one or the other opposite 5-membered ring.

The spatial arrangement of **8b**(A) and **8b**(B) in the crystal is also found in a solution of **8b** in d_6-acetone. The observed coupling patterns of the four H-atoms at the ternary C-atoms at 600 MHz allows, in combination with the corresponding ^{13}C-NMR spectrum and decoupling experiments, an unequivocal assignment of their position in the two cyclopenta[*cd*]azulene units at the central C–C bond. Irradiation of the signal of H–C(8a) (δ 3.49) caused a strong signal enhancement for H–C(2'a) (δ 5.10) and weak enhancements for those of H–C(2a) and H–C(8'). One the other hand, irradiation of the signal of H–C(4a) (δ 3.28) gave again a strong enhancement of the signal of H–C(2'a). Finally, irradiation of the signal of H–C(2a) (δ 3.17) led to medium effects on the signals of H–C(6') (δ 6.61) and H–C(2'a). All ^{1}H-NOE measurements together speak for a preferred conformation of **8b** in d_6-acetone which is close to that found in its crystal structure.

The reaction 6-*tert*-butylazulene (**1c**) with ADM is of interest since it led only to one product, namely the C(3),C(8')-dimer **5c**, which was isolated in good yield (*Scheme 4*). The difference with respect to the formation of **6b** indicates that steric interaction of substituents on the azulene reactant influences strongly the peripheral C–C bond formation, a fact which speaks for the primary formation of the central C(2a^1)–C(2'a^1) bond followed by peripheral bond formation (see later)[5]).

The results of the reaction of 5,7-dimethyl- and 5,7-diisopropylazulene (**1d** and **1e**, respectively) under our standard conditions with ADM are displayed in *Scheme 5*. At first glance, it is remarkable that we found only the maleates (*Z*)-**2d** and (*Z*)-**2e** in the reaction mixture, which speaks for a pre-orientation of ADM alongside the azulene C(2),C(6)-axis in the presence of the *Lewis* acid Et_2AlCl, so that the substituents at C(5) and C(7) sterically hinder the formation of the corresponding fumarates. Also of interest is the fact that both

---

[5]) Dimer **6c** is thermally quite stable, however, at 170° in tetralin, it undergoes an intramolecular disproportionation reaction, by which two H-atoms jump from one part of the molecule to the other (see *Scheme 3* and *Figure 1* in [13]).

azulenes gave no isolable amounts of the C(8),C(6')-dimers **5d** and **5e**. On the other hand, whereas the C(3),C(8')-dimer is formed in minor amounts in the case of **6d**, it represents the sole product in the case of **6e**. However, more astonishing is the observation that ^{i}Pr substituents suppress almost completely the formation the symmetric C(8),C(8')-dimer **7e**, whereas Me substituents at the same place favor decisively the formation of the analogous dimer **7d**. The latter one gave crystals suitable for an X-ray diffraction analysis (*Figure 3*). The central C(2a^1)–C(2'a^1) bond exhibits an almost normal length of 154.7(2) pm, but the longest peripheral bond length (C(8)–C(8'): 162.4(2) pm) observed in any of the dimers of the discussed type.

Scheme 5

Figure 3

With the intention of completing our understanding of dimer formation between azulenes and acetylenedicarboxylates under catalysis of Et_2AlCl, we investigated also reactions of 1-methylazulene (**1f**) and those with further alkyl substituents at the 7-membered ring. Results with **1f** and its 6-methyl variant **1g** are compiled in *Scheme 6*. The transformation of **1f** with ADM or ADI delivered again the corresponding C(8),C(6')-dimers **5f** and **5'f**, respectively, as main products beside small amounts of the C(3),C(8')-dimers **6f**, as well as its corresponding tetraisopropyltetracarboxylate **6'f**. The structure of **5f** was finally established by an X-ray crystal structure analysis (*Figure 4*). A further compound of the product mixture of **1f** and ADM turned out to be tetramethyl 7,11-dimethyl-3a,5a-dihydro-3*H*-3,10-(metheno)cyclopenta[*c*]azulene-1,2,4,5-tetracarboxylate (**9f**), which we isolated in a small amount and which represents obviously the *Diels-Alder* adduct of C(3)=C(4)–C(4a)=C(2a^1) of the primary addition product 4,6-Me_2-**C** (*Scheme 1*) with a second molecule of ADM (see later). Azulene **1g** behaved similarly to **1f** in the presence of ADM and the catalyst in that it formed the C(8),C(6')-dimer **5g** as the main product, accompanied by small amounts of the C(3),C(8')-dimer **6g**.

Scheme 6

Figure 4

Further results with azulenes, modified by variation of the position and bulkiness of the substituents, are collected in *Scheme 7*. They show again the dominant role of a ^{t}Bu group at C(6) in azulene **1h** for dimer formation (→ **6h**). On the other hand, azulene **1i** with Me groups at C(1,5,7) gives a quite similar product mixture to azulene **1d** with no Me group at C(1). Remarkable again is that only maleate (*Z*)-**2i** was found under the formed products (*cf.* former remarks). Catalysis experiments with **1i** and ADB under the usual conditions gave only a small amount of **7'l** beside (*E*)- and (*Z*)-**2'i**. In other words, ADM is by far the best reactant for azulenes under *Lewis* acid catalysis, followed by ADI, and then ADB.

Scheme 7

The last open question was that of the influence of an alkyl group at C(2) of the azulenes on the product pattern after reaction with ADM/Et_2AlCl under the standard conditions. The results, which, in general, were disappointing, are shown in *Scheme 8*. Quite large amounts of the corresponding fumarates and maleates (**2j** – **2l**) were isolated, whereas the yields of dimers were low, whereby only those of the C(8)–C(6') type (**5j** and 5**k**) and C(3)–C(8')-type (**5j** – **5l**) were found. It seems that the primarily formed tropylium-like intermediates of the 2-methylazulenes **1j** – **1l** are slightly longer-lived than those formed from the other azulenes **1a** – **1i**, so that the ring closure with C(8) becomes slower, thereby favoring the protonation, which leads to the observed fumarates and maleates **2**.

Scheme 8

This reasoning is supported by the astonishing results, which we realized in the Et_2AlCl catalyzed reaction of 2,5,7-trimethylazulene (**1m**) with ADM under our standard conditions (*Scheme 9*). Most amazing is the fact that we isolated from the reaction mixture only bisethenylated products such as (*E*,*E*)-**10m** and (*Z*,*E*)-**10m** in small amounts. The expected product of **1m** and ADM, in view of our former findings with 5,7-dialkylazulenes (*Scheme 5* and *7*), *i.e.*, dimethyl 2-(2,5,7-trimethylazulen-1-yl)maleate ((*Z*)-**2m**), was not found. However, we detected it as element of the C_2-symmetric C(8),C(8')-dimer (*Z*,Z)-**7m**, which was the main product in the reaction of **1m** with ADM. The other found

C(8),C(8')-dimer was of the same type, however, with one "maleic" and one "fumaric" ester side chain at C(4) and C(4'), respectively. As a last compound in the product "cocktail", we identified **11m** with the H-atoms at C(1) and C(8a) in a *cis*-relationship. The precursor is surely 3,6,8-Me_3-**C** (*cf. Scheme 1*), whereby the 1,3-H shift C(2a) → C(1) could principally take place in a concerted suprafacial manner[6]).

Scheme 9

We assume that the first ethenylation of **1m** with ADM leads predominantly to the corresponding maleate, as observed in the other cases with alkyl substituents in the 5,7-position of the azulene. The second ethenylation of the maleate at C(3) with ADM is retarded, due to the presence of the strong π-acceptor substituent at C(1), and leads mainly to ring closure with C(4), so that the maleate-carrying analog of 3,6,8-Me_3-**C** can undergo the Et_2AlCl catalyzed dimerization to yield (*Z*,*Z*)-**7m**. The 2-(2,5,7-trimethylazulen-1-yl)fumarate formed in smaller amounts is, after addition of ADM, also engaged in the dimerzation reaction with the maleate-carrying analog to yield the "mixed" dimer (*Z*,*E*)-**7m**[7]).

The results discussed so far indicate the scope and limitation of dimer formation from azulenes and acetylenedicarboxylates *via* type **C** intermediates under acid catalysis. The analysis of the reaction of the 1-methylazulenes **1f** – **1i** (*Schemes 6* and *7*) showed that the formed dimers are derived from the attack of ADM on C(3) and C(4) of the azulenes, so that they carry the Me group at C(4) and C(4'), respectively. In the case of **1f**, we found, as already mentioned, a minor amount of the tetracyclic tetracarboxylate **9f**, the structure

---

[6]) AM1 calculations give for (1*RS*,8a*RS*)-**11m** $\Delta H_f° = -74.37$ Kcal·mol^{-1}. Its stereoisomer (1*SR*,8a*RS*)-**11m** shows $\Delta H_f° = -78.65$ Kcal·mol^{-1}. The difference of –4.28 Kcal·mol^{-1} speaks for a [1,3s]-H jump across the present 10 π-electron systems taking into account that its precursor 3,6,8-Me_3-**C** is by 1.1 Kcal·mol^{-1} richer in energy than (1*RS*,8a*RS*)-**11m**.

[7]) However, we cannot exclude that, in the present case, ((*Z*) → (*E*))-isomerization took place in the course of Et_2AlCl-catalysis.

of which indicates also the primary addition of ADM at C(3) and C(4) of **1f**. As a consequence of these findings, we subjected a number of azulenes with Me groups at C(1) and C(3) to the reaction with ADM under our standard conditions. The results were unambiguous (*Scheme 10* and *11*). The dimer formation is completely suppressed and tetracyclic tetracarboxylates of the type, which we had found already in the reaction of **1f** as side product **9f**, are now dominant (*cf.* **1n** - **1p** and **1r**). A comparison of the results of the reaction of **1o** and **1q** shows that the remote ^{t}Bu group in the case of **1q** exerts a certain steric hindrance in that side products are also formed. (*Z*)-**11p** and (*Z*)-**4p** could be expected as follow-up products of the corresponding primary intermediate of type **C** (*cf. Scheme 2*). The formation of compound (*Z*)-**11'p**, found in small amounts, is still not clear[8]).

3. **Thermal Behavior of the Heptacyclic Dimers Formed from Azulenes and Acetylenedicarboxylates**. – Table 2 gives a survey of the central σ-bond lengths of the four observed dimer types **5**, **6**, **7**, and **8** taken from the X-ray crystal structures already mentioned in Section 2, together with the corresponding AM1 calculated values for the basic skeletal structures **5α**, **6α**, **7α,** and **8α**. The calculated σ-C,C bond length are 1 – 4% shorter. However, the relative deviation Δd within the individual structures is almost the same with the exception of **7d**/**7α** due to the Me substituents at the peripheral C(8)–C(8') bond of **7d**. Since we observed the easy H^+ catalyzed cleavage of the peripheral C(8)–C(6') bond of **5b** resulting in a disproportionation of the cyclopenta[*cd*] azulene units and formation of **8b**, we studied the thermal

[8]) A possible source of (*Z*)-**11'p** could be (*Z*)-**11p**. Despite the fact that its H–C(2a^1) is ideally disposed for H^- abstraction by carbocations such as Ph_3C^+ or Me_3C^+, we got no results on treatment of (*Z*)-**11p** with these carbocations, followed by quenching with water. It might also be that it is the corresponding type **C** intermediate that already looses H^- from C(8a) in the course of the catalysis with Et_2AlCl. The intervention of O_2 from the air can be excluded, since the reactions were performed under pure N_2.

behavior of dimers of type **5** in toluene at 70 – 100° and found that they all rearranged more or less cleanly to the corresponding type **8** dimers, which were obtained as sole products in 40 – 90% yield after chromatographic purification and re-crystallization (Table 3).

Table 2

Table 3

A casual observation led to further experiments. When we tried to purify dimer **5'f** by sublimation at $4 \cdot 10^{-2}$ bar, we noticed that its bright orange crystals already turned blue before melting (124.7 – 125.2°). In the present case, the appearance of a blue color indicates in general the formation of an azulene derivative. Therefore, we repeated the experiment with **5'f** and its methyl ester variant **5f** under low vacuum at 185 – 200°. The results are shown in *Scheme 12*[9]).

Scheme 12

Indeed, the blue component, which we observed visually, turned out to be diisopropyl 4-methyl-3,4-dihydrocyclopenta[*cd*]azulene-1,2-dicarboxylate (4-Me-**E**') and its methyl ester variant 4-Me-**E** in lower yield. Dimers **7f** and **7'f**, which were not formed in the Et_2AlCl catalyzed reaction of the corresponding azulenes with ADM and ADI, respectively (*Scheme 6*), could be identified spectroscopically, since we had isolated this type of C_2 symmetric dimers with other azulenes (see, *e.g.*, *Scheme 3* as well as Table 1). Most interesting was the new second product type, represented by **14f** and **14'f**, since they showed the same number of signals in the NMR spectra and with similar coupling patterns as **7f** and **7'f** (Table 4), findings from which followed conclusively that these compounds stand for C_2 symmetric structural isomers of the latter. Their structures were finally established by an X-ray crystal structure analysis of **14'f** (*Figure 5*).

---

[9]) The reaction with **5'f** was repeated in decalin at 175°, in order to be able to follow its thermal transformation by TLC. In this case, the only product that could be isolated was **14'f** in a yield of 29%. None of the reactions described in *Scheme 12* and *13* were optimized systematically.

Table 4

Figure 5

Further heating experiments with the (2a^1,2'a^1)-dimers **5b**, **5'b**, and **8g** are displayed in *Scheme 13*. They showed that heating in decalin gave in all three cases the corresponding (8,8')-dimers **7** and (5,5')-dimers **14** accompanied by varying amounts of the 1,2-dihydrocyclopenta[cd]azulene-1,2-dicarboxylates of type **C** with the ester substituents in a *trans*-relationship[10]).

Scheme 13

4. Mechanistic Considerations. – 4.1. *Acid Catalyzed Reactions*. The experiments with azulenes and acetylenedicarboxylates (ADR) under acid catalysis, discussed in the preceding section, demonstrate that the interaction of both reactants takes place principally in two steps, whereby the first step represents an electrophilic substitution of the azulenes at C(1) (or C(3)) by the ADR·acid complex. This opens two reaction channels for the second step, which is characterized by loss of H^+, thus leading to the formation of (azulen-1-yl)fumarates and -maleates or ring closure to form 2a,8a-dihydrocyclopenta[*cd*]azulene-1,2-dicarboxylates (**C**; *Scheme 1*).

The most interesting finding is that the latter structures dimerize under H^+-catalysis already at low temperature to form three type of dimers **5** – **7**, which all possess a central σ-bond between C(2a^1)–C(2'a^1) but varying lateral σ-bonds between C(8)–C(6'), C(3)–C(8'), and C(8)–C(8'), respectively (*Scheme 3*). The amounts of these dimers formed, depend on the substituents at the azulenes and to a lesser extent also on the alkyl groups of ADR.

The formation of the three dimer types may also be influenced by the heat of formation ($\Delta H_f°$) of their basic C-skeletons. The AM1 calculated values (Kcal·mol^{-1}) are 188.95 (C(8),C(6')), 195.53 (C(3),C(8')) and 196.15 (C(8),C(8')), respectively. These values are principally in good agreement with the amounts of **5a**, **6a**, and **7a**, which we have found in the case of azulene

---

[10]) ^3J(H–C(1),H–C(2)) = 2.4 Hz (E = COO^{i}Pr) and 2.8 – 3.0 Hz (E = COOMe).

itself (*Scheme 3*). Nevertheless, the formation of the dimers under acid catalysis takes place under kinetic control[11]).

Since we also observed formation of **5a** and **6a** in the presence CF_3COOH in decalin at room temperature [12], we believe the Et_2AlCl catalyzed reactions are H^+ catalyzed too, because Et_2AlCl already contains traces of HCl at the start or HCl is transiently formed by re-aromatization of azulenium ions resulting from electrophilic attack of the $Et_2AlCl{\cdot}ADR$ onto the azulene. The possible ways that H^+ can catalyze the formation of the dimers of type **5** – **7**, are displayed in *Scheme 14*. The cross-conjugated π-system of intermediates of type **C** can principally be protonated at C(3) or C(8), which yields the corresponding cross-conjugated ternary carbonium ions. These ions seem to interact with C(2a) of a second molecule **C,** whereby the charge is shifted to the linearly conjugated heptatrienylium ions **F** and **G,** which contain already the C(2a)–C(2'a) bond. The thus obtained spatial closeness of the two former **C** structures allows then the formation of the lateral σ-bonds again under shift of the charge to yield **5a**-H^+ and **7a**-H^+ on one side and **6a**-H^+ on the other side.

Scheme 14

The two reaction channels leading finally to dimers of type **5**/**7** and of type **6**, respectively, is in general agreement with the fact that protonation of intermediates of type **C** at the five-membered ring leads to a larger ring strain relief than that at the seven-membered ring (Fig. 6)[12]). Indeed, the product ratio in the case of azulene (**1a**) amounts to (**5a** + **7a**) : **6a** = 4.3 (*Scheme 3*).

---

[11]) The acid catalyzed cleavage of the lateral C(8)–C(6') bond of **5b** and **5'b** under H-migration and formation of **8b** and **8'b** is in perfect agreement with the corresponding AM1 calculated $\Delta H_f°$ values of the "naked" C-skeletons (see [4])).

[12]) It might also be of interest to note that 2,2a,2a[1],4a-tetrahydrocyclopenta-[*c*,*d*]azulene and 2a,2a[1],4a,5-tetrahydrocyclopenta[*cd*]azulene with the H-atom at H–C(2a[1]) in an *anti*-relationship to those in a *syn*-postion at C(2a) and C(4a) show according to AM1 calculations $\Delta\Delta H_f°$ = 4.2 Kcal·mol^{-1} in

Fig.6

This ratio can be disturbed substantially by steric effects exerted by substituents on the azulene, as demonstrated by the acid catalyzed dimerization of **1b** and **1c** (*Scheme 4*). In the case of **1b**, one finds a ratio (**5b** + **7b**) : **6b** ≈ 5, whereas in the case of **1c** only **6c** is found in a respectable yield beside larger amounts of (*E*)- and (*Z*)-**2c**. All these observations support the mechanism of H^+ catalysis of **C** type intermediates as proposed in *Scheme 14*.

4.2. *Thermal Reaction of Dimers* **5** *and* **8**. It was astonishing for us to observe that on heating in toluene at 70 – 100° only type **5** dimers underwent a smooth rearrangement to dimers **8** by cleavage of their lateral C(8)–C(6') bond accompanied by an H-shift (*Table 3*). The smoothness of this cleavage and H migration speaks for a concerted process. Indeed, the X-ray crystal structure of **5a** (*Fig. 1*), as well as its AM1 calculated C-skeleton, shows H–C(8'a) well below C(4a) (*d*(AM1) = 229 pm); *d*(X-ray) = 232 pm), so that it can jump onto C(4a) under concomitant cleavage of C(8)–C(6') and migration of C(4a)=C(5) and C(6)=C(7). In other words, the observed lateral bond cleavage is part of an intramolecular concerted bisvinylogous retro-ene reaction.

The conformational freedom around the C($2a^1$)–C($2'a^1$) bond creates three local minima and two of them have the 7-membered rings almost above each other, so that the above-discussed bisvinylogous retro-ene process can be reverted at temperatures above 170°, thus leading to the C_2 symmetric dimers of type **7** and **14** (see *Scheme 12* and *13*). Of interest is the fact that the dimers of type **14** are not involved in the click cascade of bond formations of azulenes and acetylenedicarboxylates under H^+-catalysis at 0 – 20°.

The financial support of this work by the *Swiss National Science Foundation* is gratefully acknowledged.

---

favor of the former structure. H–C($2a^1$) mimics in both cases C($2'a^1$) of a second moiety **C**.

Experimental Part

All experimental details for the syntheses can be found in [12][13] and especially in the Ph.D. work of Yi Chen (University of Zurich, 1993) and of Erja Anneli Lehto (University of Zurich, 1997).

Since short hand notation is used for dimers of types **5**, **6**, and **7**, we give here the systematic IUPAC names, generated with ACD/Name (ACD/Labs, Toronto) of the three dimers **5a**, **6a**, and **7a** (*Scheme 3*).

5a: tetramethyl (2a*R**,8a*R**,10a*S**,11*R**,12*R**,14*S**)-2a,8a,10a,11,12,14a-hexahydro-12,5-(metheno)-11,6-(prop[1]en[1]yl[3]ylidene)cycloocta[1,2-*c*:4,3-*c'*]dipentalene-1,2,9,10-tetracarboxylate;

6a: tetramethyl (3a*R**,5*S**,6*R**,7*S**,9a*R**)-3a,5a,6,7,7a,9a-hexahydro-7,14-(metheno)-6,1-(prop[1]en[1]yl[3]ylidene)cyclohepta-[*j*]cyclopenta[*l*]-as-indacene-4,5,8,9-tetracarboxylate;

7a: tetramethyl (3a*R**,5a*S**,6*R**,7*R**,7a*S**,9a*R**)-3a,5a,6,7,7a,9a-hexahydro-6,1:7,12-diprop[1]en[1]yl[3]ylidenedicyclopent[*j,l*]-as-indacene-4,5,8,9-tetracarboxylate.

X-ray Crystal Structure Determinations for Compounds **5a**, **5f**, **7d**, **8b**, *and* **14'f** (see *Table 5* and *Figs. 1-5*) [13]). All measurements were conducted at low-temperature on a *Rigaku AFC5R* diffractometer [15] fitted to a 12kW rotating anode generator with graphite-monochromated Mo$K\alpha$ radiation (λ = 0.71073 Å). The intensities for each structure were corrected for *Lorentz* and polarization effects, but not for absorption. The data collection and refinement parameter are given in *Table 5*, views of the molecules are shown in *Figs. 1-5.*

Each structure was solved by direct methods using SHELXS-86 [16], which revealed the positions of all non-H-atoms. In **8b**, there are two molecules in the asymmetric unit. The only significant differences between the independent

---

[13]) CCDC–1059876-1059880 contain the supplementary crystallographic data for this paper. These data can be obtained free of charge from The Cambridge Crystallographic Data Centre via www.ccdc.cam.ac.uk/data_request/cif.

molecules are the orientations of the ester groups. The four ester groups in molecule A, containing atoms O(1), O(3), O(5) and O(7), differ in orientation from the corresponding groups in molecule B by approximately 170°, 175°, 33° and 15°, respectively. In all other respects the conformations of the molecules are identical.

The non-H-atoms of each structure were refined anisotropically. All of the H-atoms were placed in geometrically calculated positions and refined by using a riding model where each H-atom was assigned a fixed isotropic displacement parameter with a value equal to $1.2U_{eq}$ of its parent atom ($1.5U_{eq}$ for the methyl groups). Each structure was refined on F^2 by using full-matrix least-squares procedures, which minimised the function $\Sigma w(F_o^2 - F_c^2)^2$. A correction for secondary extinction was applied in the case of **14'f**. In the cases of **5a**, **5f**, and **8b**, 19, 5 and 4 reflections, respectively, whose intensities were considered to be extreme outliers, were omitted from the final refinements. Neutral atom scattering factors for non-hydrogen atoms were taken from [17a], and the scattering factors for H-atoms were taken from [18]. Anomalous dispersion effects were included in F_c [19]; the values for f' and f'' were those of [17b]. The values of the mass attenuation coefficients were those of [17c]. The *SHELXL-2014* program [20] was used for all calculations. The crystallographic diagrams were drawn using ORTEPII [21].

REFERENCES

[1] H.-J. Hansen, *Chimia* **1996**, *50*, 489 and **1997**, *51*, 147.

[2] K. Abou-Hadeed, H.-J. Hansen, in 'Science of Synthesis' Georg Thieme Verlag KG, Stuttgart–New York, 2010, Vol. 45b, p. 1043.

[3] a) K. Hafner, H. Diehl, H.U. Süss, *Angew. Chem.* **1976**, *88*, 121; b) H.J. Lindner, B. Kitschke, *Angew. Chem.* **1976**, *88*, 123.

[4] K. Hafner, G.L. Knaup, H.J. Lindner, *Bull. Chem. Soc. Jpn.* **1988**, *61*, 155.

[5] Y. Chen, R.W. Kunz, P. Uebelhart, R.H. Weber, H.-J. Hansen, *Helv. Chim. Acta* **1992**, *75*, 2447.

[6] Y. Chen, H.-J. Hansen, *Helv. Chim. Acta* **1993**, *76*, 168.

[7] P. Uebelhart, H.-J. Hansen, *Helv. Chim. Acta* **1992**, *75*, 2493.

[8] A. Magnussen, P. Uebelhart, H.-J. Hansen, *Helv. Chim. Acta* **1993**, *76*, 2887.

[9] F.K. Kläner, B. Dogan, W.R. Roth, K. Hafner, *Angew. Chem.* **1982**, *94*, 721.

[10] a) R.-A. Fallahpour, H.-J. Hansen, *High Pressure Research* **1992**, *11*, 125;
b) R.-A. Fallahpour, H.-J. Hansen, *Helv. Chim. Acta* **1995**, *78*, 1933.

[11] A. Linden, M. Meyer, P. Mohler, A.J. Rippert, H.-J. Hansen, *Helv. Chim. Acta* **1999**, *82*, 2274 – 2315

[12] P. Brügger, P. Uebelhart, R.W. Kunz, R. Siegrist, H.-J. Hansen, *Helv. Chim. Acta* **1998**, *81*, 2001.

[13] P. Uebelhart, E. Lehto, H.-J. Hansen, *Heterocycles* **2014**, *88*, 521.

[14] L. A. Paquette, C.C. Liao, R.I. Burson, R.E. Wingard, Jr., C.N. Shih, J. Fayos, J. Clardy, *J. Am. Chem. Soc.* **1977**, *99*, 6935.

[15] MSC/AFC Diffractometer Control Software, Molecular Structure Corporation, The Woodlands, Texas, 1991.

[16] G.M. Sheldrick, *Acta Crystallogr., Sect. A* **1990**, *46*, 467.

[17] a) E.N. Maslen, A.G. Fox, M.A. O'Keefe, in 'International Tables for Crystallography', Ed. A.J.C. Wilson, Kluwer Academic Publishers, Dordrecht, 1992, Vol. C, Table 6.1.1.1, pp. 477-486; b) D.C. Creagh, W.J. McAuley, *ibid*. Table 4.2.6.8, pp. 219-222; c) D.C. Creagh, J.H. Hubbell, *ibid*. Table 4.2.4.3, pp. 200-206.

[18] R.F. Stewart, E.R. Davidson, W.T. Simpson, *J. Chem. Phys.* **1965**, *42*, 3175.

[19] J.A. Ibers, W.C. Hamilton, *Acta Crystallogr.* **1964**, *17*, 781.

[20] G.M. Sheldrick, *Acta Crystallogr., Sect. C* **2015**, *71*, 3.

[21] C.K. Johnson, ORTEPII, Report ORNL-5138, Oak Ridge National Laboratory, Oak Ridge, Tennessee, 1976.

Received March 31, 2015

Table 1. *^{1}H-NMR Shifts and ^{1}H,^{1}H Couplings of C(8,6') Dimer* **5a**, *C(3,8') Dimer* **6a**, and *C(8,8') Dimer* **7a**[a])

5a				**6a**			**7a**		
Pos.	δ(H)	Mult.	*J* (Hz)	δ(H)	Mult.	*J* (Hz)	δ(H)	Mult.	*J*(Hz)
C(2a)	3.40	*t*-like	2.8, Σ 5.8[b])	2.93	*dd*	3.5, <0.8	3.38	*t*-like	Σ 6.3[h])
C(2'a)	4.08	*t*-like	3.0, Σ 5.9[c])	3.22	*t*-like	Σ 6.14[d])			
C(3)	6.44	*dd*	5.5, 2.9	3.64	*t*-like	Σ 7.17, <1[e])	6.25	*dd*	5.6, 3.0
C(3')	6.51	*dd*	5.5, 3.0	6.34	*dd*	5.5, 3.1			
C(4)	6.36	*d*	5.5	5.99	br. *d*	3.1	6.30	*d*	5.6
C(4')	6.32	*d*	5.7	6.41	*d*	5.5			
C(5)	6.13	*d*	7.4	6.59	*d*	11.5	6.02	*d*	7.5
C(5')	6.31	*d*	8.3	6.14(1)	*d*	7.3			
C(6)	6.11	*dd*	11.1, 7.9	5.90	*dd*	11.5, 7.3	6.05	*dd*	10.8, 7.7
C(6')	3.66 – 3.59	*m*		6.25	*dd*	11.6, 7.6			
C(7)	5.52	*dd*	11.0, 6.6	6.13	*dd*	11.5, 7.7	5.89	*dd*	11.0, 6.7[i])
C(7')	5.29	*ddd*	11.6, 9.5, 2.2	6.14(3)	*dd*	11.5, 7.5			
C(8)	3.66 – 3.59	*m*		5.88	*dd*	11.6, 8.0	3.17	*ddt*-like	6.7, 3.5[j])
C(8')	5.28	*d*	11.6	3.25	*dt*-like	7.7, Σ 7.9[f])			
C(8a)	3.66 – 3.59	*m*		3.56	*dd*	8.2, 3.7	3.48	*t*-like	Σ 6.9[k])
C(8'a)	4.40	*q*-like	≈ 2.5	3.49	*t*-like	Σ 7.4[g])			

[a]) 600 MHz (**5a**) and 400 MHz (**6a** + **7a**) in $CDCl_3$; $CHCl_3$ at 7.260 ppm.

[b]) $\Sigma = {}^3J$(H–C(2a), H–C(3)) + ${}^4J$(H–C(2a), H–C(8a)); ${}^4J$(H–C(2a), H–C(8a)) = 2.8.

[c]) $\Sigma = {}^3J$(H–C(2'a), H–C(3')) + ${}^4J$(H–C(2'a), H–C(8'a)); ${}^4J$(H–C(2'a), H–C(8'a)) = 3.0.

[d]) $\Sigma = {}^3J$(H–C(2'a), H–C(3')) + ${}^4J$(H–C(2'a), H–C(8'a)).

[e]) $\Sigma = {}^3$J(H–C(3), H–C(4)) + ${}^3J$(H–C(3)), H–C(8')); ${}^3J$(H–C(3)), H–C(2a)) <1.

[f]) $\Sigma = {}^3J$(H–C(8'), H–C(8'a)) + ${}^3J$(H–C(8')), H–C(3)); ${}^3J$(H–C(8'), H–C(7')) = 7.7.

[g]) $\Sigma = {}^3J$(H–C(8'a), H–C(8')) + ${}^4J$(H–C(8'a), H–C(2'a)).

[h]) $\Sigma = {}^3J$(H–C(2a/2'a), H–C(3/3')) + ${}^4J$(H–C(2a/2'a), H–C((8a/8'a)).

[i]) ${}^3J$(H–C(7/7'), H–C(6/6')) and ${}^3J$(H–C(7/7'), H–C(8/8')).

[j]) ${}^3J$(H–C(8/8'), H–C(7/7')) and ${}^3J$(H–C(8/8'), H–C(8a/8'a)); ${}^4J$(H–C(8/8'), H–C(6/6')) and ${}^5J$(H–C(8/8'), H–C(5/5')) <1.

[k]) $\Sigma = {}^3J$(H–C(8a/8'a), H–C(8/8')) + ${}^4J$(H–C(8a/8'a), H–C(2a/2'a)).

Table 5. *Crystallographic Data for Compounds* **5a**, **5f**, **7d**, **8b**, *and* **14'f**

	5a	**5f**	**7d**	**8b**	**14'f**
Crystallised from	CH_2Cl_2 / *n*-hexane	CH_2Cl_2 / Et_2O	MeOH / CH_2Cl_2	Et_2O / *n*-hexane	CH_2Cl_2 / Et_2O
Empirical formula	$C_{32}H_{28}O_8$	$C_{34}H_{32}O_8$	$C_{36}H_{36}O_8$	$C_{34}H_{32}O_8$	$C_{42}H_{48}O_8$
Formula weight [g mol^{-1}]	540.54	568.62	596.65	568.59	680.84
Crystal colour, habit	colourless, prism	colourless, prism	colourless, prism	orange, prism	colourless, prism
Crystal dimensions [mm]	0.20 × 0.38 × 0.45	0.20·0.35·0.50	0.15 × 0.20 × 0.50	0.30 × 0.33 × 0.50	0.25 × 0.25 × 0.48
Temperature [K]	173 (1)	173 (1)	173 (1)	173 (1)	173 (1)
Crystal system	monoclinic	monoclinic	triclinic	triclinic	monoclinic
Space group	$P2_1/c$	$P2_1/c$	$P\bar{1}$	$P\bar{1}$	$C2/c$
Z	4	4	2	4	4
Reflections for cell determination	21	25	23	22	25
2θ range for cell determination [°]	37 – 40	38 – 40	35 – 40	39 – 40	35 – 40
Unit cell parameters a [Å]	7.190 (5)	7.870 (5)	9.590 (2)	8.580 (2)	18.515 (2)
b [Å]	23.073 (5)	22.991 (4)	10.0479 (19)	19.045 (7)	10.614 (2)
c [Å]	15.480 (5)	15.586 (2)	16.775 (3)	19.150 (7)	18.845 (2)
α [°]	90	90	80.169 (14)	108.30 (3)	90
β [°]	98.51 (4)	102.75 (2)	87.562 (17)	96.78 (3)	101.623 (7)
γ [°]	90	90	69.503 (16)	102.59 (3)	90
V [Å^3]	2540 (2)	2750 (2)	1491.6 (5)	2840.2 (17)	3627.5 (7)
F(000)	1136	1200	632	1200	1456
D_x [g cm^{-3}]	1.414	1.373	1.328	1.330	1.247
μ(Mo $K\alpha$) [mm^{-1}]	0.102	0.0970	0.0932	0.0940	0.0851
Scan type	$\omega/2\theta$	$\omega/2\theta$	$\omega/2\theta$	$\omega/2\theta$	$\omega/2\theta$
$2\theta_{(max)}$ [°]	55	60	60	55	55
Total reflections measured	6247	8731	9235	13363	4274
Symmetry independent reflections	5838	8015	8690	12972	4152
R_{int}	0.057	0.075	0.022	0.025	0.016
Reflections with $I > 2\sigma(I)$	4071	5645	6439	9897	3143
Reflections used in refinement	5819	8010	8690	12968	4152
Parameters refined	365	385	405	769	232
$R(F)$ [$I > 2\sigma(I)$ reflections]	0.0435	0.0497	0.0523	0.0495	0.0459
$wR(F^2)$ [all reflections]	0.1234	0.1457	0.1618	0.1480	0.1248
Weighting parameters [a; b][a])	0.0368; 2.4701	0.072; 0.5615	0.0875; 0.3332	0.0836; 0.8141	0.0559; 2.3323
Goodness of fit	1.026	1.028	1.059	1.033	1.030
Secondary extinction coefficient	-	-	-	-	0.0024(4)
Final Δ_{max}/σ	0.001	0.001	0.001	0.001	0.001
$\Delta\rho$ (max; min) [e Å^{-3}]	0.32; -0.28	0.41; -0.24	0.50; -0.29	0.47; -0.27	0.35; -0.19

[a]) $w^{-1} = \sigma^2(F_o^2) + (aP)^2 + bP$ where $P = (F_o^2 + 2F_c^2)/3$

Table 2. *Length (*pm*) of the Central* σ*-Bonds of Dimer* **5a**, **6b**, **7d**, *and* **8b** *determined by X-ray Crystal Structure Analysis in Comparison with Those Calculated* by AM1 *for the Basic Structures* **5α** – **8α**

Dimer[a])	C(2a^1)–C(2'a^1)	C(8)–C(6')	C(3)–C(8')	C(8)–C(8')	Δ*d* (%)[b])
5a	159.0(3)	160.5(3)	–	–	0.9
5α[c])	154.0	155.8	–	–	1.2
6b	156.1(2)	–	161.2(3)	–	3.3
6α	152.9	–	156.8	–	2.6
7d	154.7(2)	–	–	162.4(2)	5.0
7α	152.6	–	–	157.0	2.9
8b[d])	156.7(2)	–	–	–	–
8α	154.6	–	–	–	–

[a]) Each time: first line X-ray, second line AM1.
[b]) Deviation (%) with respect to the length of C(2a^1)–C(2'a^1).
[c]) $\Delta H_f°$ (AM1; Kcal·mol^{-1}); **5α**: 188.23; **6α**: 195.53; **7α**: 188.95; **8α** 188.55 (see also footnote [4]).
[d]) Value for molecule A; for molecule B: 157.2(2)°.

Table 3. *Thermal Transformation of Dimers* **5** *into Dimers* **8** *in Toluene*[a])

Dimer	Temp. [°]	Time [h]	Dimer	Yield [%][b])
5b	70	0.5	**8b**	40
5'b	85	0.83	**8'b**	90
5f	100	1.5	**8f**	62
5'f	90	1.0	**8'f**	57
5g	90	0.83	**8g**	81

[a]) 0.05 – 0.1 M solution.
[b]) Crystallized pure products after CC (silica gel).

Table 4. *^{1}H-NMR Shifts (δ) and Coupling Constants (*Hz*) of the* C_2*-Symmetric C(8),C(8')- and C(5),C(5')-Dimers* **7b** *and* **14b**[a])

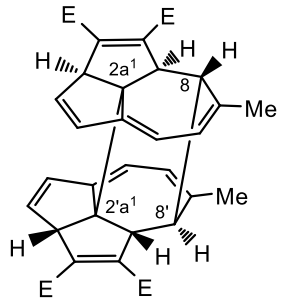

7b

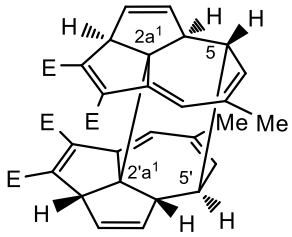

14b

Position	**7b**	**14b**
H–C(2a,2'a)	3.39 (*t*-like; 3.2, 3.1)	3.53 (*quint*-like; Σ 6.8)
H–C(3,3')	6.16 (*dd*; 5.6, 3.1))	5.81 (*dt*; 5.5, 2.0)
H–C(4,4')	6.29 (*d*; 5.6)	5.37 (*dq*; 5.5, 3.3, 1.5)
H–C(5,5')	5.95 (*d*; 8.1)	3.00 (*dd*, 7.3, 3.4)
H–C(6,6')	5.87 (*dd*; 8.1,1.2)	5.87 (*dd*; 7.8, 1.3)
Me–C(7,7')	1.79 (*d*; 1)	1.91 (*s*)
H–C(8,8')	2.94 (*d*; 3.4)	6.03 (*d*; 1.3)
H–C(8a,8'a)	3.46 (*t*-like; 3.5, 3.2)	2.90 (*m*)
E–C(1,1',2,2')	3.72, 3.65 (2 *s*)	3.87, 3.73 (2 *s*)

[a]) 300 MHz spectra in $CDCl_3$; E = COOMe.

Text to Figures

Fig. 1. *Stereoscopic view of the X-ray crystal structure of dimer* **5a** (50% probability ellipsoids)

Fig. 2 *Stereoscopic view of the X-ray crystal structure of dimer* **8b** (molecule A of the two symmetry-independent molecules shown; 50% probability ellipsoids)

Fig. 3 *Stereoscopic view of the X-ray crystal structure of dimer* **7d** (50% probability ellipsoids)

Fig. 4 *Stereoscopic view of the X-ray crystal structure of dimer* **5f** (50% probability ellipsoids)

Fig. 5 *Stereoscopic view of the X-ray crystal structure of dimer* **14'f** (50% probability ellipsoids)

Fig. 6 *Stereoscopic view of the AM1 calculated structures of* **C** *and its C(3)- and C(8)-protonated forms* (Θ stands for the bond angles; their sum (Σ) indicates the non-planarity of the structures)

Scheme 1

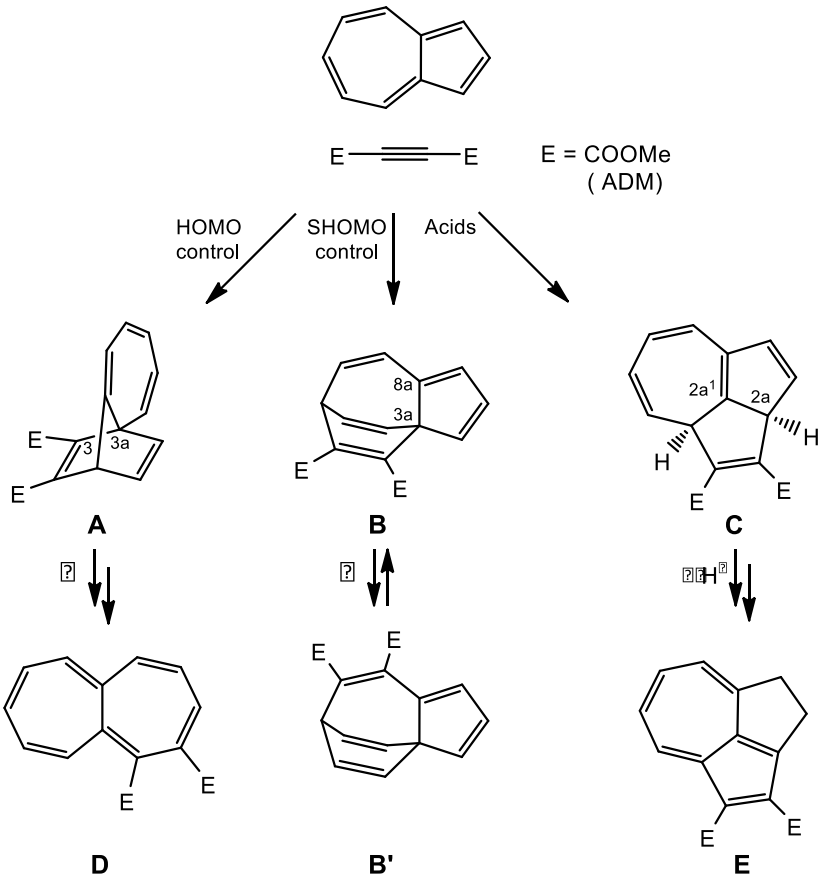
E
E
E = COOMe
(ADM)
HOMO
control
SHOMO
control
Acids
E
3
3a
E
A
8a
3a
E
E
B
2a1
2a
H
H
E
E
C
E
E
D
E
E
B'
E
E
E

Scheme 2[a])

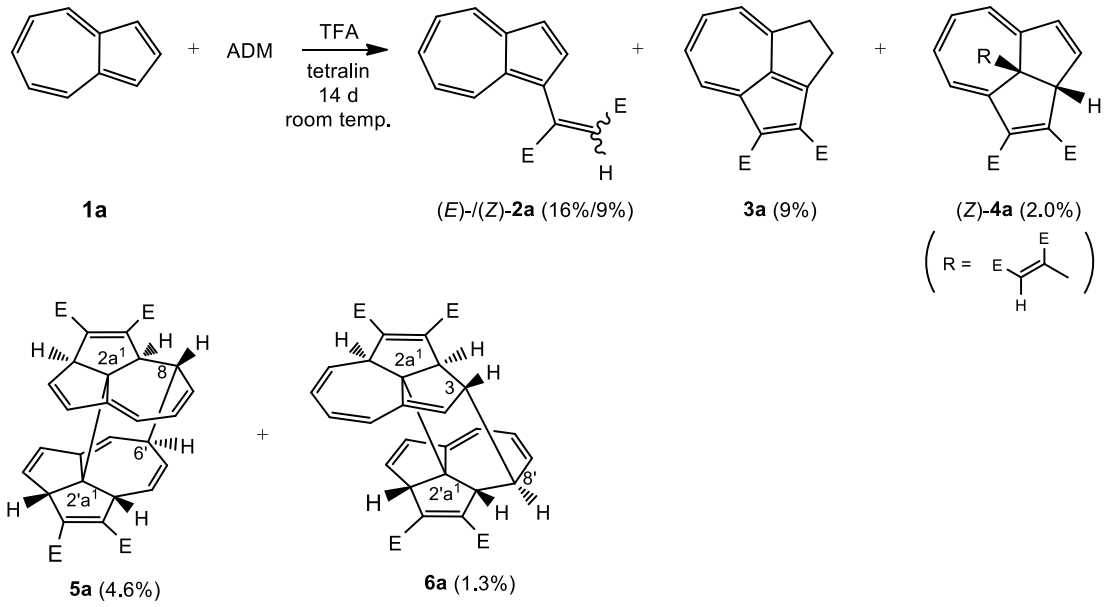

[a]) Taken from [10]. For two further complex products, see *Scheme 5* in [10].

Scheme 3

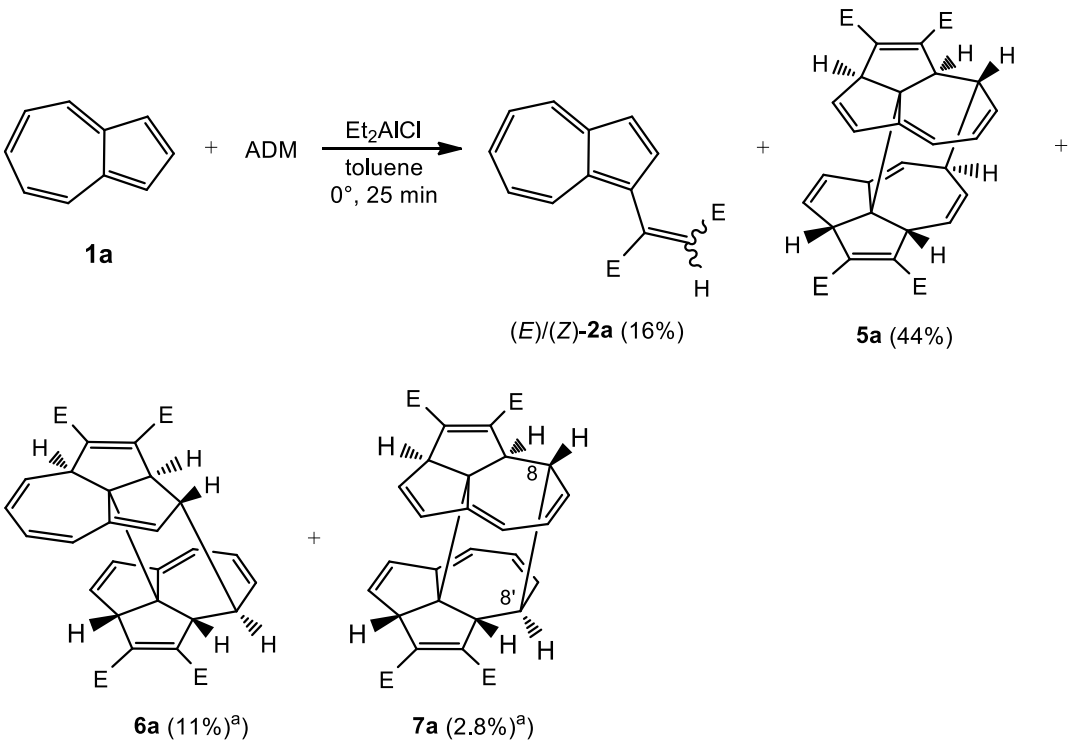

1a

(*E*)/(*Z*)-**2a** (16%)

5a (44%)

6a (11%)[a])

7a (2.8%)[a])

[a]) Heptacycles **6a** and **7a** were isollated as a 4:1 mixture.

Scheme 4

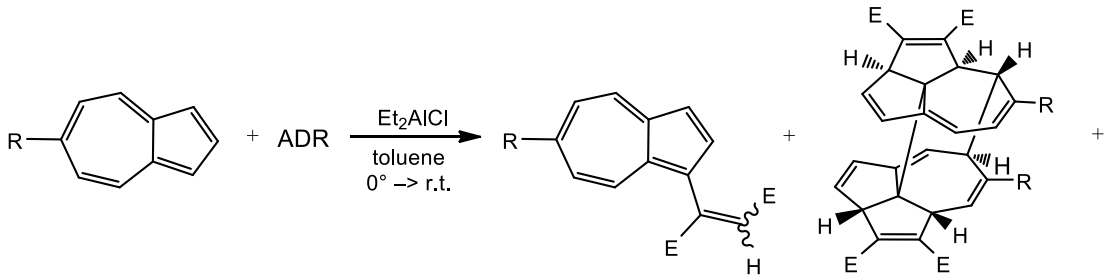

R = Me: **1b** (ADM) **1b** (ADI)[b]) R = ^{t}Bu: **1c** (ADM)[c])

(*Z*)-**2b** (5.3%; 5.8%)[a]) (*E*)/(*Z*)-**2'b** (2.5%/11%) (*E*)/(*Z*)-**2c** (15%/12%)

5b (21%; 33%) **5'b** (36%) **5c** (n.o.)

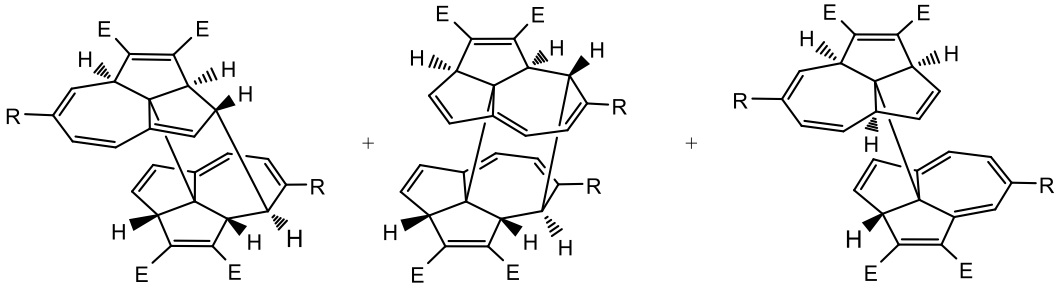

6b (11%; 0.4%) **6'b** (0.4%) **6c** (53%)

7b (2.8%; n.o.) **7'b** (n.o.) **7c** (n.o.)

8b (6.8%; 4.7%) **8'b** (4.0%) **8c** (n.o.)

---

[a]) Yield of isolated products; time: 1.5 h/1.67 h; n.o. = not observed in isolable amounts. In the second run, in addition to the displayed products, 0.3% of pure dimethyl 6-methyl-3.4-dihydrocyclopenta[*cd*]azulene-1,2-dicarboxylate (6-methyl-**E**; *cf. Scheme 1*) were isolated.

[b]) Time: 2 h.

[c]) Time: 25 min.

Scheme 5

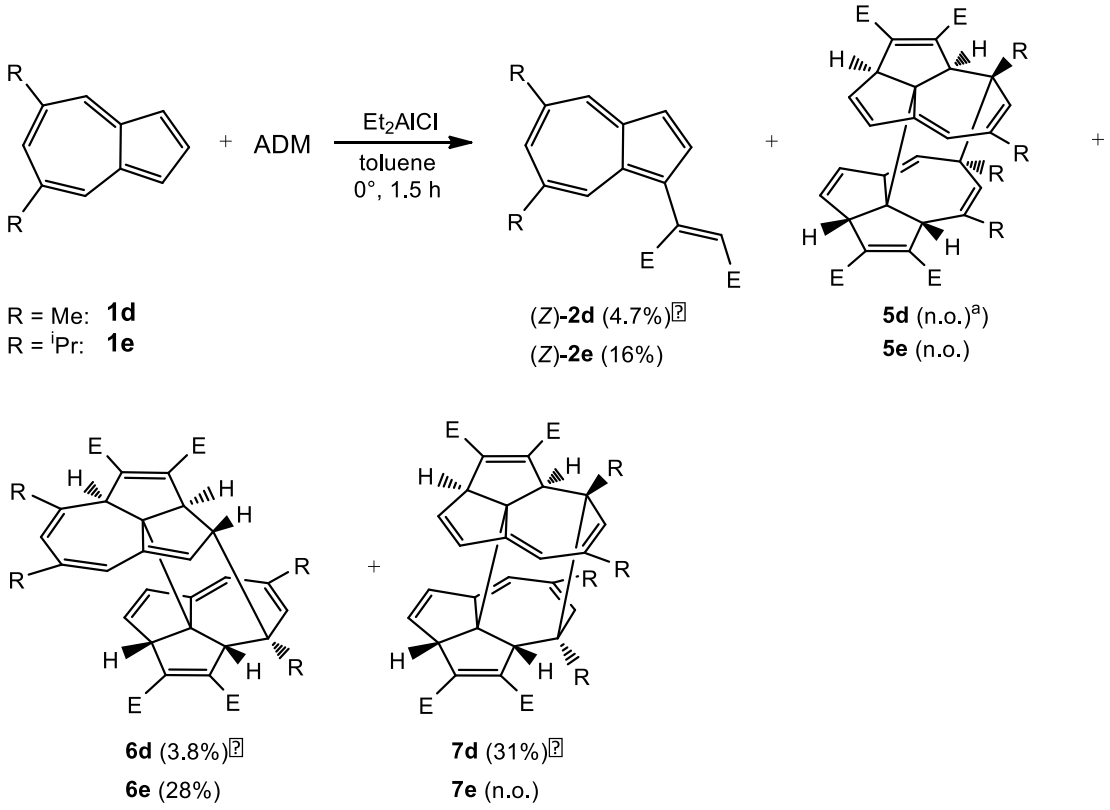

a) n.o. = not observed in isolable amounts.

Scheme 6[a])

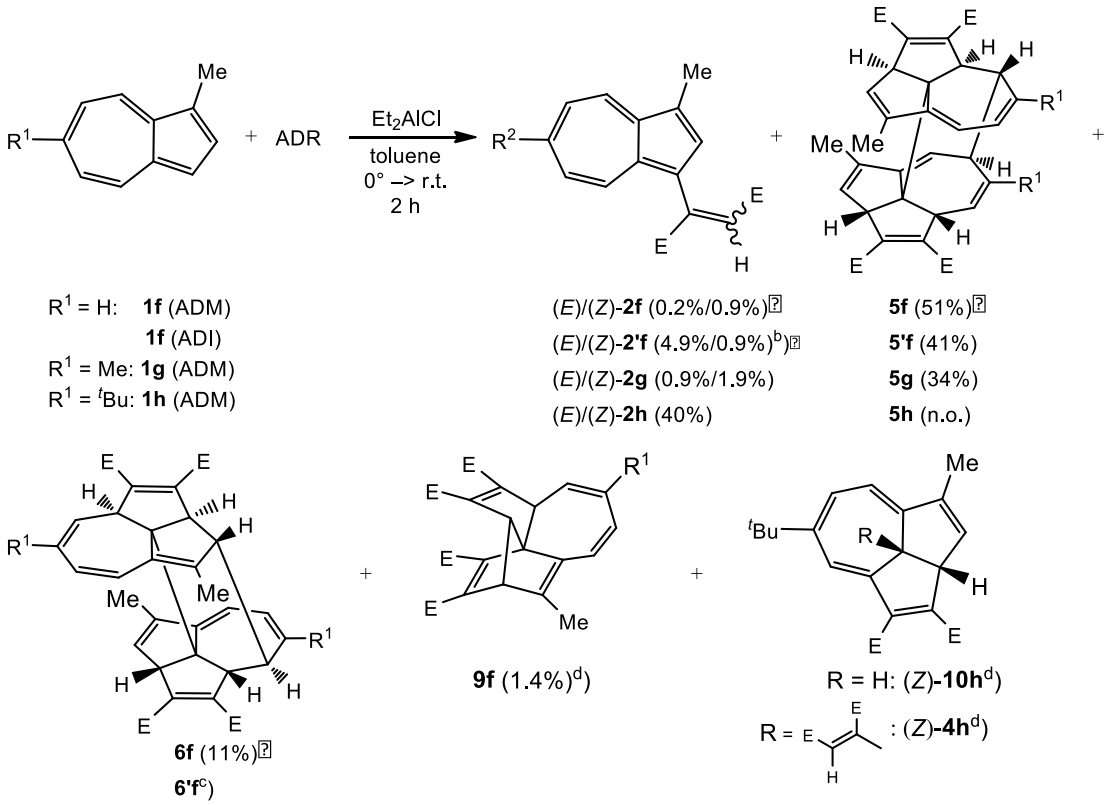

a) Products of type **7** and **8** (*Scheme 4*) were not observed.

b) In addition, 3.3% of diisopropyl (*Z*)-1-(2-methylazulen-1-yl)ethene-1,2-dicarboxylate were isolated.

c) Identified in ^{1}H-NMR spectra of mixtures, but not isolated.

d) Not observed in the analogous other cases.

Scheme 7[a])

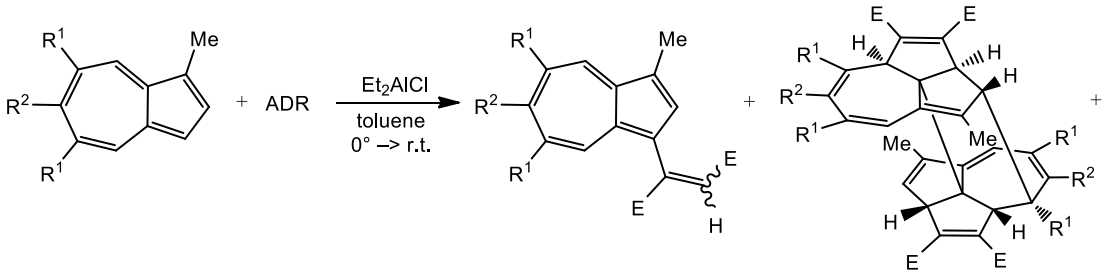

R^1 = H, R^2 = ^{t}Bu: **1h** (ADM)
R^1 = Me, R^2 = H: **1i** (ADM)
1i (ADB)

(*E*)/(*Z*)-**2h** (25%/25%)[?]
(*Z*)-**2i** (5.4%)
(*E*)/(*Z*)-**2'i** (2.9%/0.5%)

6h (47%)[?]
6i (8.5%)
6'i (n.o.)[c])

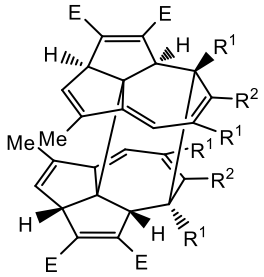

7h (n.o.)[?]
7i (34%)
7'i (7.0%)

---

[a]) Products of type **5** (*cf. Scheme 4*) were not observed.
[b]) Reaction time: 20 min (**1h**), 3.5 h (**1i**).
[c]) n.o. = not observed in isolable amounts.

Scheme 8[a])[b])

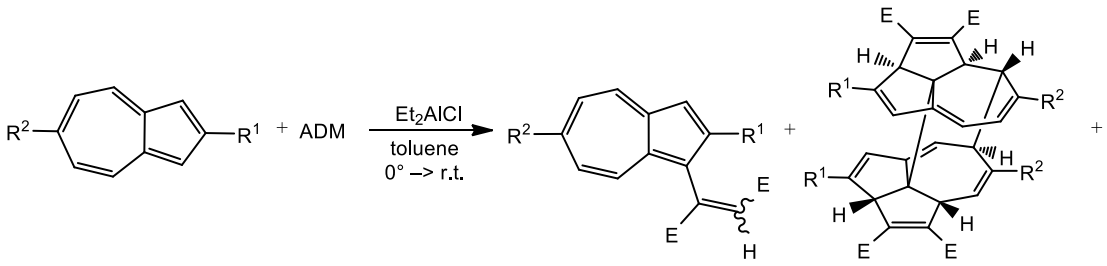

R^1 = Me, R^2 = H: **1j**
R^1 = ^{i}Pr, R^2 = H: **1k**
R^1 = R^2 = Me: **1l**

(*E*)/(*Z*)-**2j** (11%/20%)
(*E*)/(*Z*)-**2k** (11%/12%)[?]
(*E*)/(*Z*)-**2l** (15%/27%)

5j (6.2%)[?]
5k (10%)
5l (n.o.)

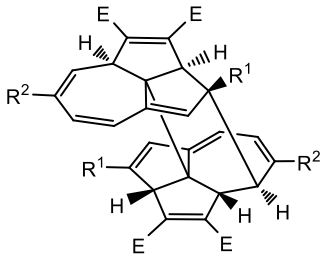

6j (12%)[?]
6k (4.1%)
6l (1.0%)

[a]) Products of type **7** and **8** (*cf. Scheme 4*) were not observed.
[b]) Reaction time: 3.3 h (**1j**), 3.5 h (**1k**), 1.5 h (**1l**).

Scheme 9

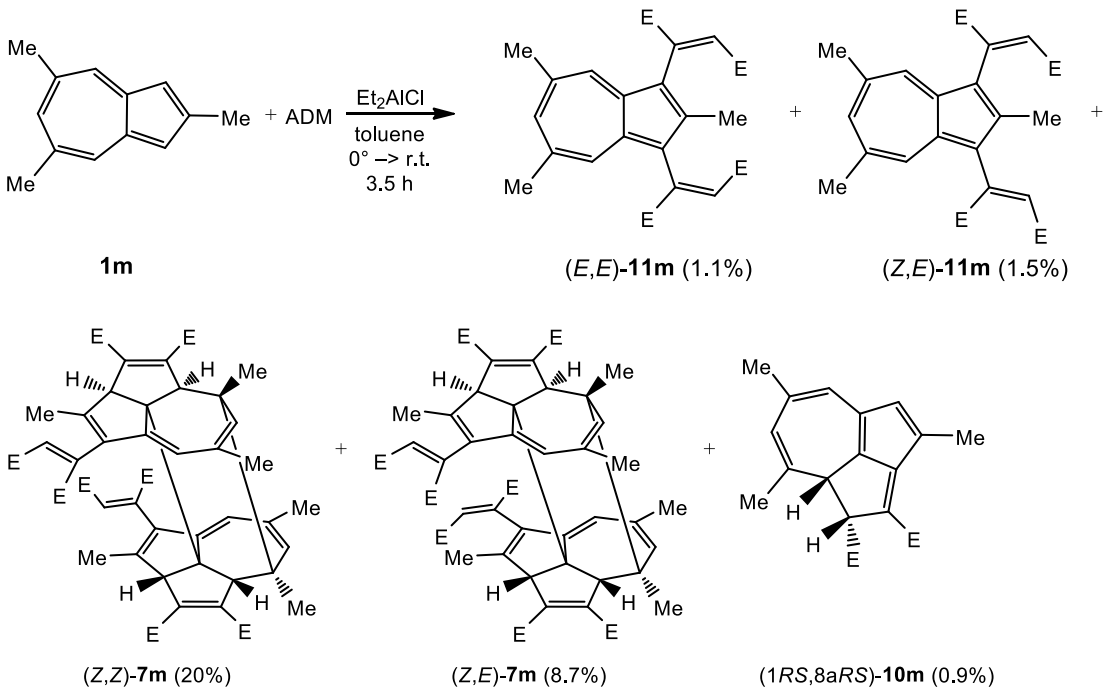
Me
Me
Me
+ ADM
Et2AlCl
toluene
0° –> r.t.
3.5 h
E
E
E
+
+
1m
(E,E)-11m (1.1%)
(Z,E)-11m (1.5%)
H
(Z,Z)-7m (20%)
(Z,E)-7m (8.7%)
(1RS,8aRS)-10m (0.9%)

Scheme 10

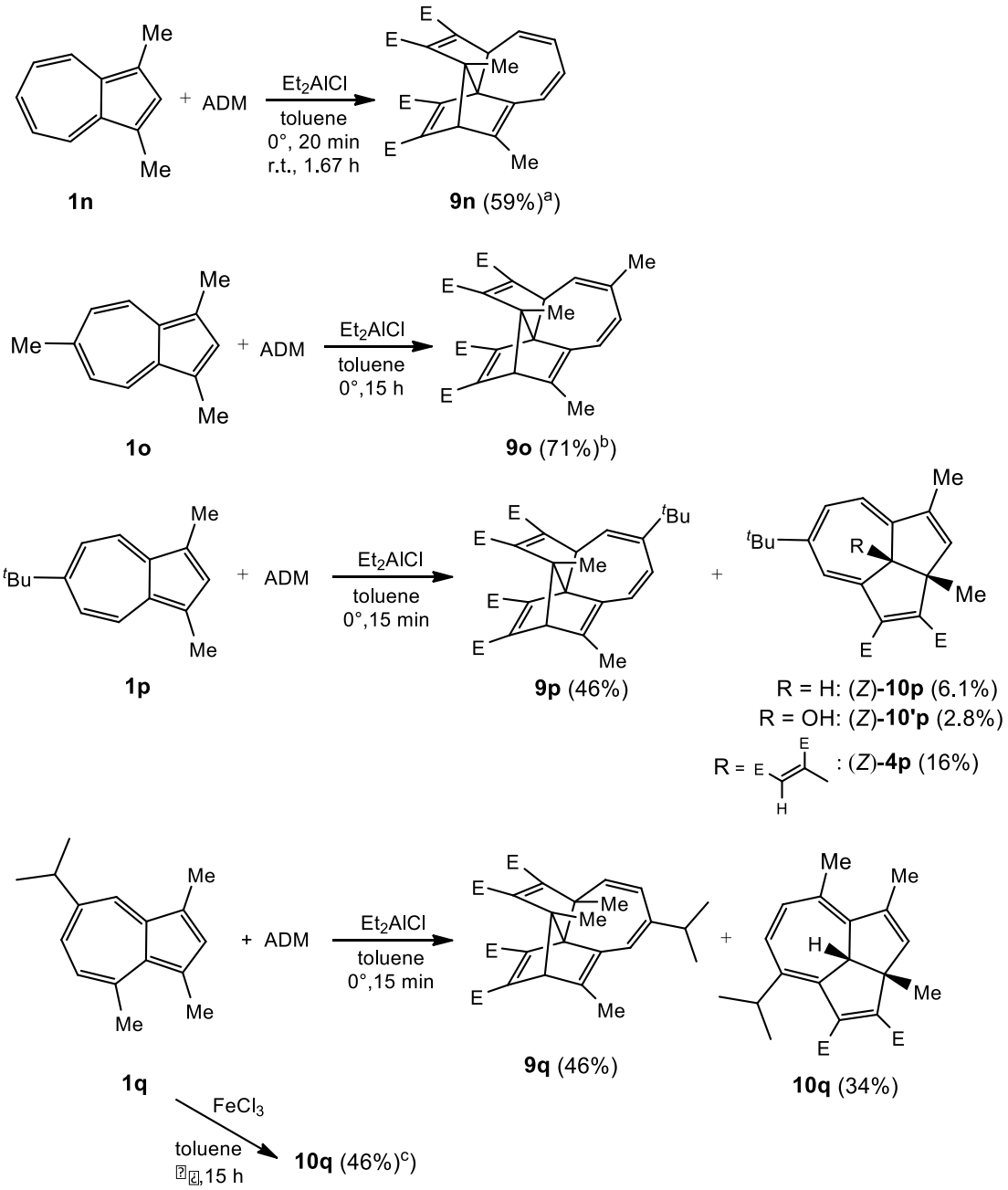

a) Yield with respect to 10% recovered **1n.**

b) Yield with respect to 15% recovered **1o.**

c) Yield with respect to 50% recovered **1q.**

Scheme 11

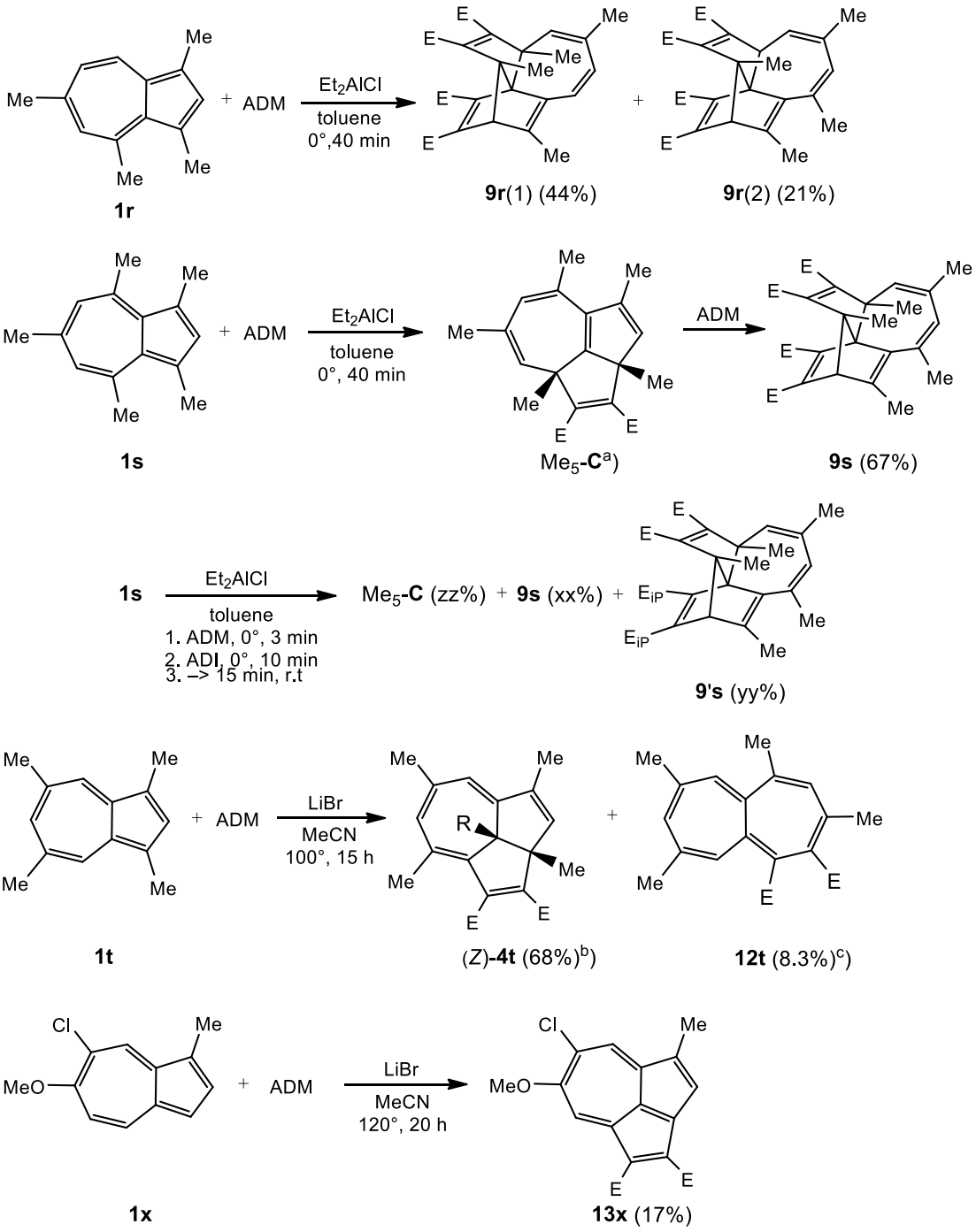

[a]) Recognized by TLC, but not isolated.

[b]) With respect to 10% recovered **1t.**

[c]) As a mixture with its double bond shifted (DBS) isomer **12't.**

Scheme 12

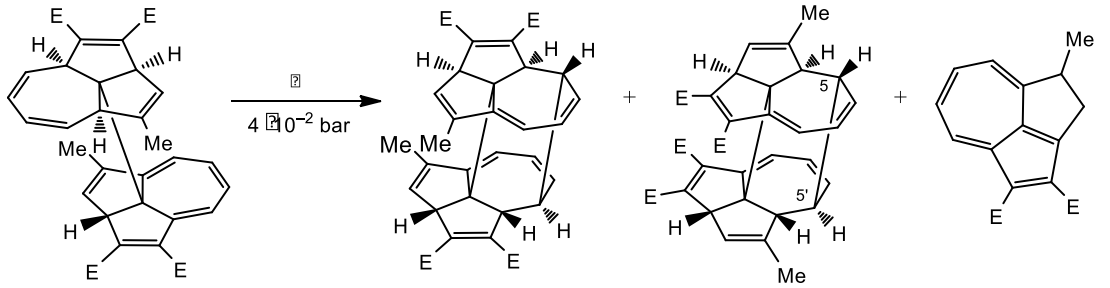

8f (E = COOMe) 200°/2.3 h **7f** (8.7%) **14f (**6.1%) 4-Me-**E** (3.3%)
8'f (E = COO^{i}Pr) 185°/1.7 h **7'f** (5.3%) **14'f** (24%) 4-Me-**E'** (17%)

Scheme 13

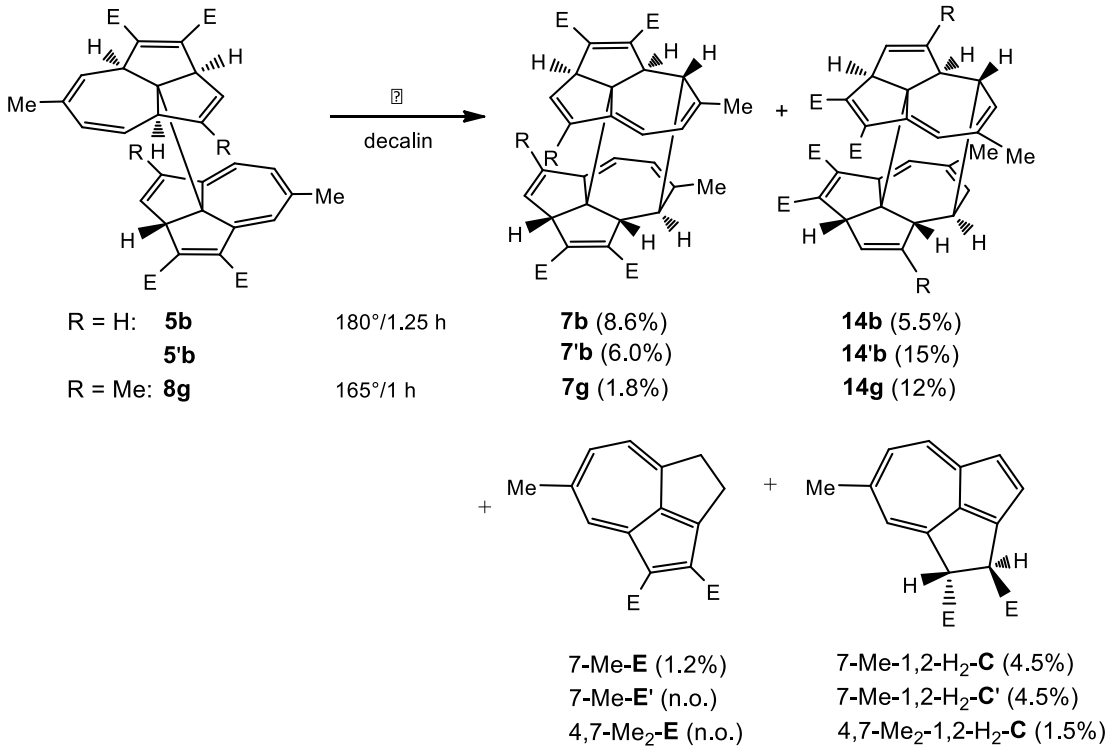
decalin
R = H: 5b
5'b
R = Me: 8g
180°/1.25 h
165°/1 h
7b (8.6%)
7'b (6.0%)
7g (1.8%)
14b (5.5%)
14'b (15%)
14g (12%)
7-Me-E (1.2%)
7-Me-E' (n.o.)
4,7-Me2-E (n.o.)
7-Me-1,2-H2-C (4.5%)
7-Me-1,2-H2-C' (4.5%)
4,7-Me2-1,2-H2-C (1.5%)

Scheme 14

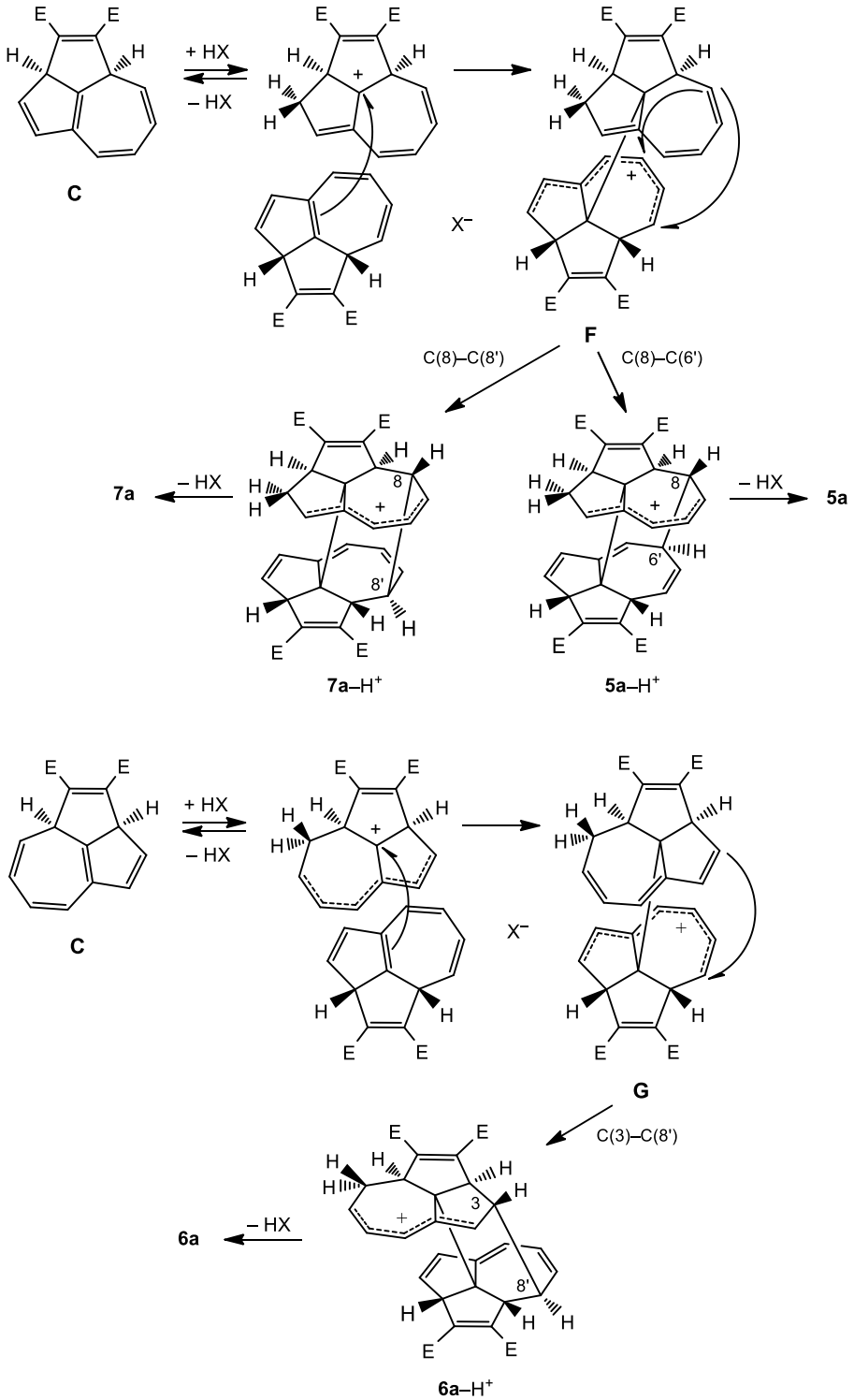

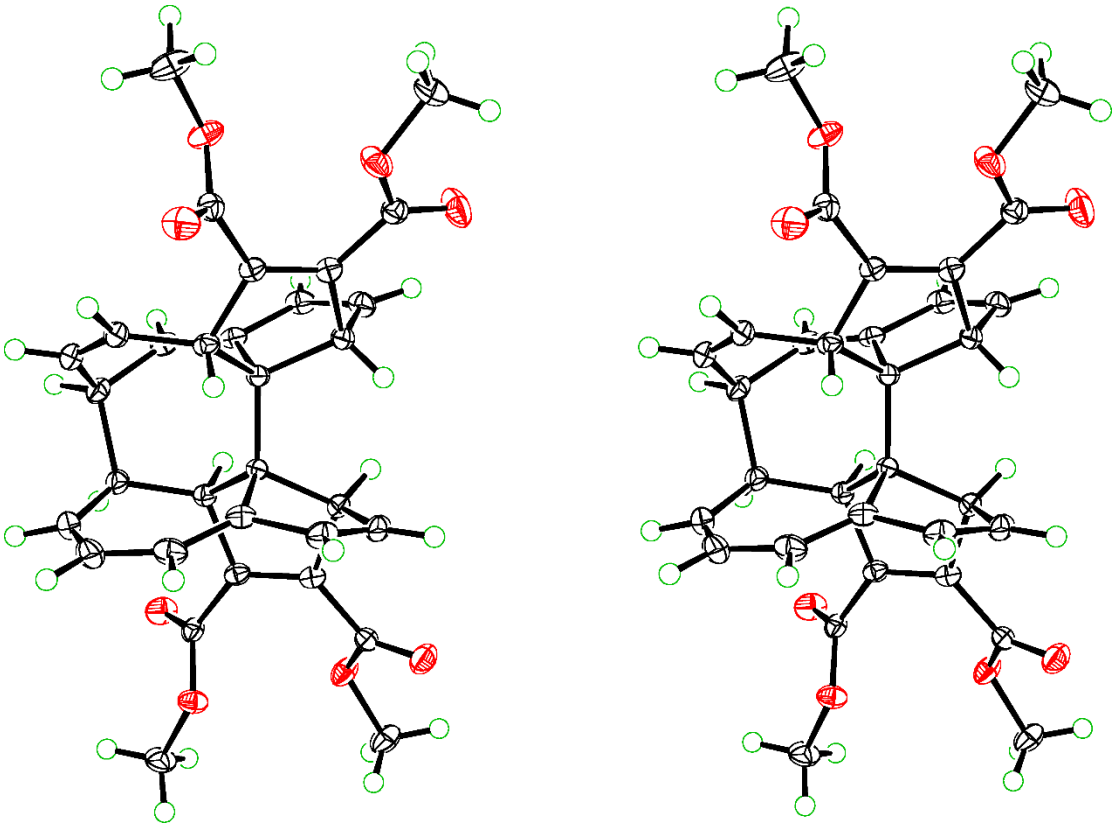

Fig. 1

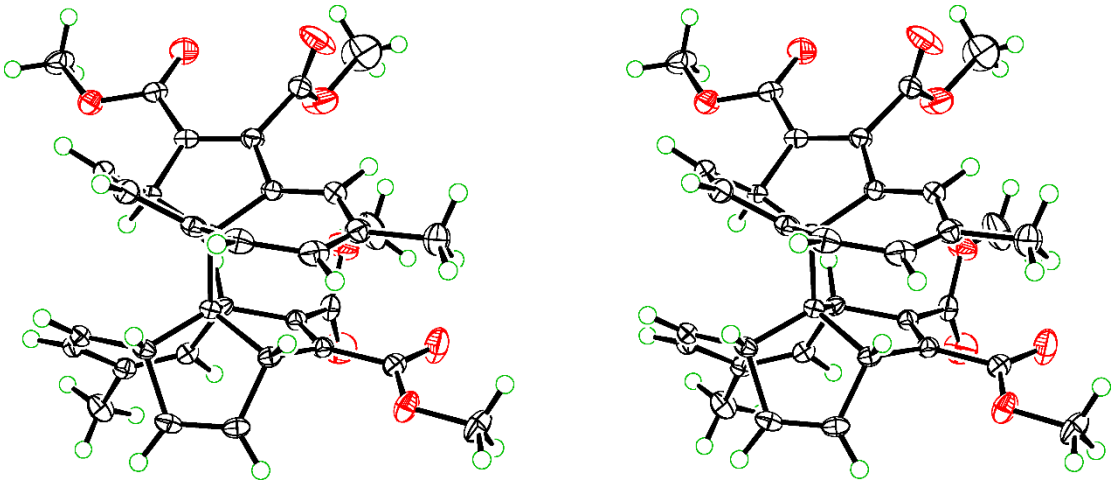

Fig. 2

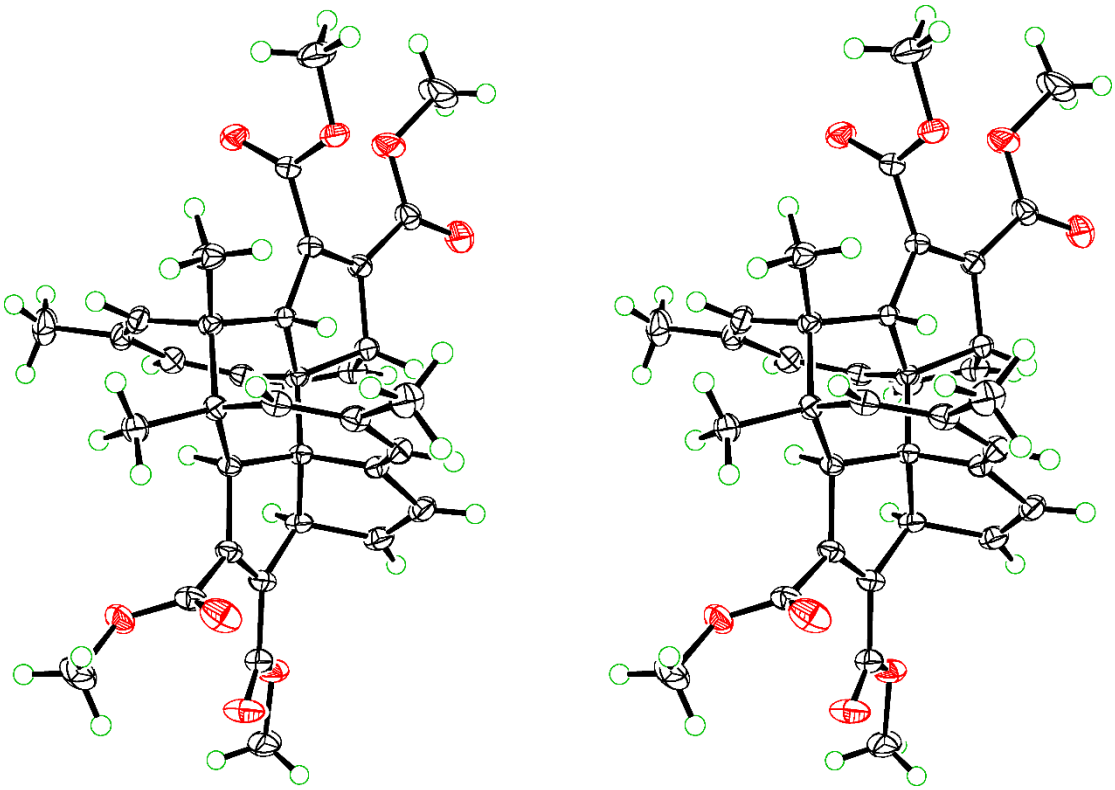

Fig. 3

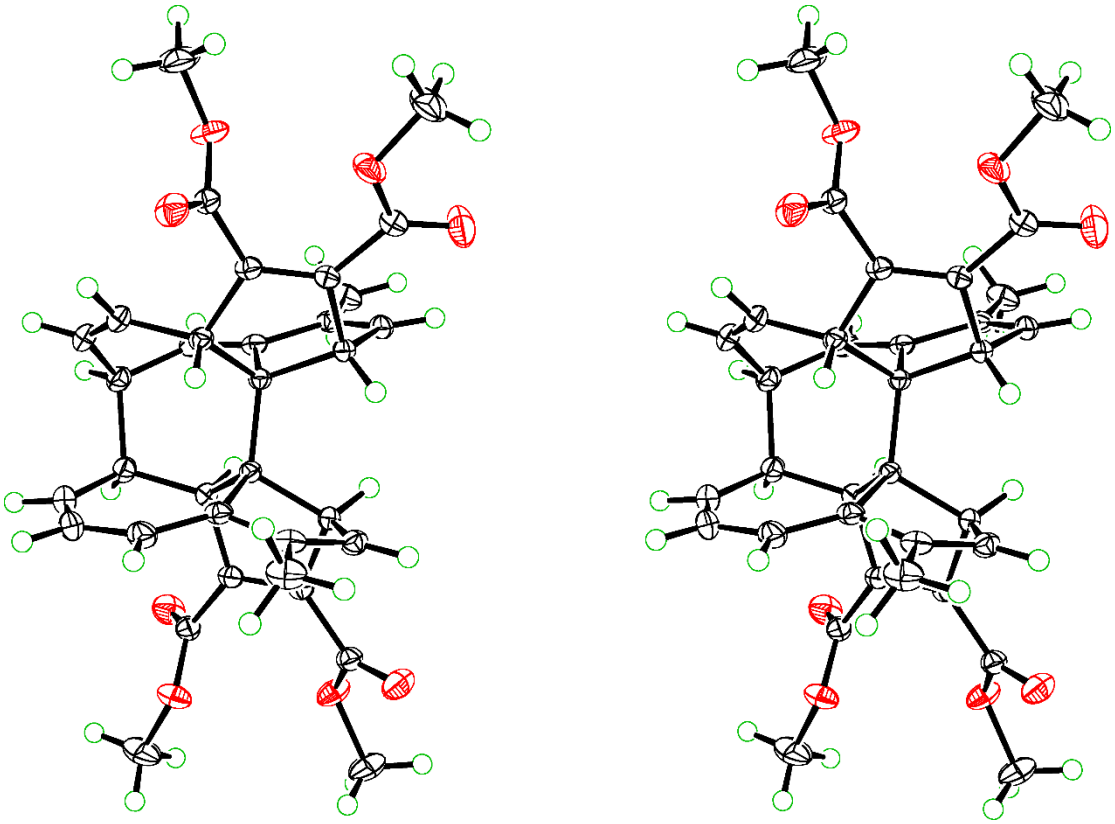

Fig. 4

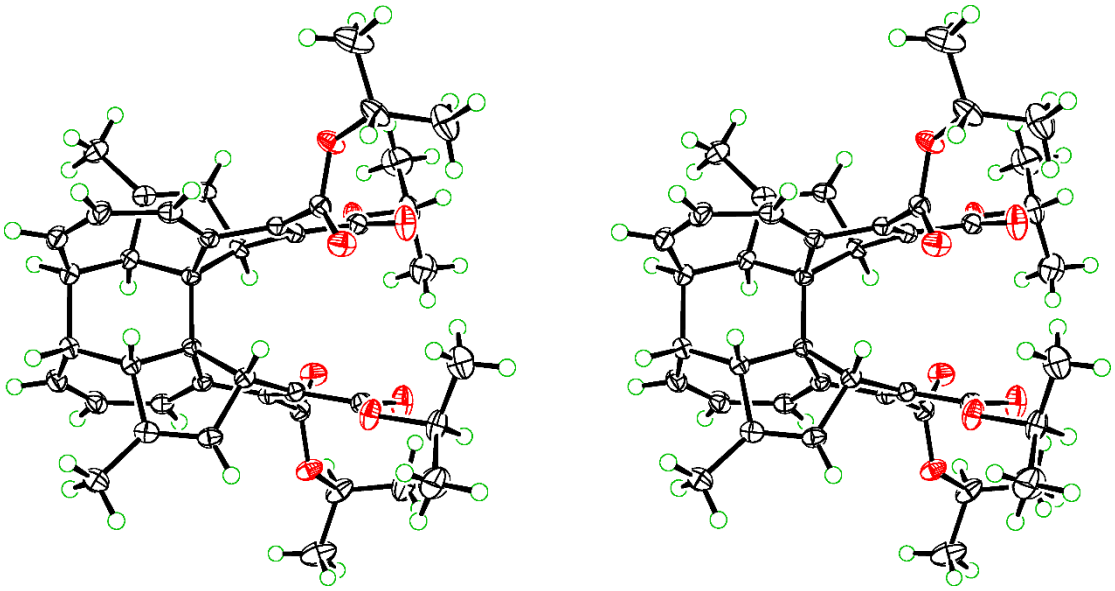

Fig. 5

2a,8a-dihydrocyclopenta[*cd*]azulene[a])

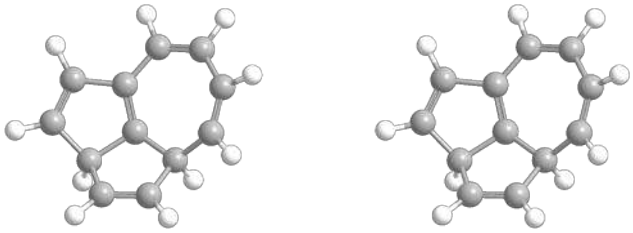

$\Delta H_f°$ = 106.35 Kcal·mol^{-1}

$\Sigma\ \Theta(2a^1)$ = 355.4°

C(3)- Prot.

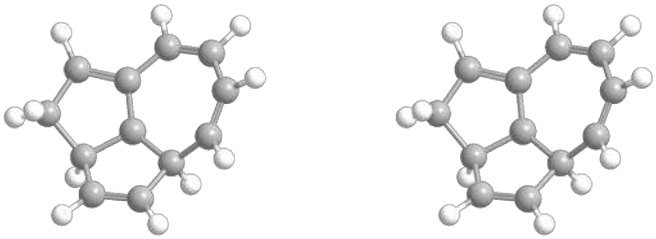

$\Delta H_f°$ = 267.12 Kcal·mol^{-1}

$\Sigma\ \Theta(2a^1)$ = 357.0°

C(8)-Prot.

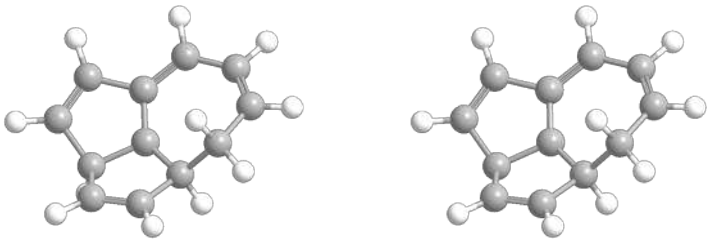

$\Delta H_f°$ = 269.46 Kcal·mol^{-1}

$\Sigma\ \Theta(2a^1)$ = 356.3°

Fig. 6